High Haematocrit Blood Flow and Adsorption of Micro and Nanoparticles on an Atherosclerotic Plaque: An *In-silico* Study

Mohamadamin Forouzandehmehr[1,2] and Amir Shamloo[1,*]

[1]*School of Mechanical Engineering, Sharif University of Technology, Tehran, Iran;* [2]*Faculty of Medicine and Health Technology, Tampere University, Tampere, Finland*

Abstract: ***Background*:** The continuing inflammatory response entailed by atherosclerosis is categorised by a pathological surface expression of certain proteins over the endothelium, namely, P-selectins. Thus, to boost the efficiency of drug carriers, these proteins can be used as binding targets.

***Method*:** An *in-silico* patient-specific model of a Left Anterior Descending (LAD) coronary artery considering the luminal unevenness was built and meshed using the finite element method.

***Objectives*:** Delivery of particles in a specific size range, from 200 to 3200 nm, covered by P-selectin aptamers (PSA), to an atherosclerotic plaque in a pathologically high haematocrit (Hct) blood flow was simulated. The surface of the plaque was assumed to possess a pathologically high expression of P-Selectins.

***Results*:** The distribution of deposited particles over the plaque in high Hct blood was significantly more homogenous compared to that of particles that travelled in normal blood Hct. Moreover, in the high Hct, the increase in the particle size, from 800 nm forwards, had a trivial effect on the upsurge in the surface density of adhered particles (SDAs) over the targeted endothelium. Yet, in normal blood Hct (45% in this research), the increase in the particle diameter from 800 nm forwards resulted in a significant increase in the SDAs over the targeted plaque. Interestingly, unlike the adsorption pattern of particles in normal Hct, a significant distribution of deposited particles in the post-constriction region of the atherosclerotic plaque was observed.

***Conclusion*:** Our findings provide insights into designing optimum carriers of anti-thrombotic/inflammatory drugs specifically for high blood Hct conditions.

Keywords: high haematocrit, nano drug carriers, adhesion, personalised modelling, atherosclerotic plaque.

1. INTRODUCTION

Endothelial Cell (EC) dysfunction and inflammation are linked to the upsurge of certain adhesion proteins on the pathologic locations [1]. As a well-known example, P-Selectins can be assumed as a promising target to achieve site-specific treatments using nano-drug carriers [2]. The invasive structure of conventional treatments and their considerable restenosis risk necessitate the employment of new treatment approaches. Applying nanocarriers as a non-invasive method for tracing the diseased endothelium can play a key role in the improvement of the diagnosis and treatment of inflammation-originated disease, namely the atherosclerotic plaques. Quite a few investigations have employed different targeting binding peptides or antibodies to prove the capability of this method in the detection of organ transplant rejection, angiogenesis, atherosclerotic plaque, and myocardial ischemic memory [2-6].

*Address correspondence to this author at the School of Mechanical Engineering, Sharif University of Technology, Tehran, Iran;
E-mail: shamloo@sharif.edu

The geometrical properties of the arterial network and atherosclerotic lesions of every person are unique. Correspondingly, age, genetic factors, and anatomical structure affect the biodistribution, metabolism, and clearance of drugs and their biochemistry on the target cells. Remarkably, multi-scale mathematical modelling in nanomedicine is a key factor in the development of future personalised treatments [7-10]. In this context, computer-based simulations have played a key role in many biomedical fields such as cardiac cell studies, blood-brain barriers (BBB), and tissue engineering [11-14]. Importantly, applying the patient specificity approach in medicine has been reflected as an accomplished tool to better understanding numerous indices in pharmacology and haemodynamics, namely, biomarker evaluations and the standardisation of personalised high-end computing algorithms [15-17].

Instead of assuming constant affinity in the receptor-mediated adhesion, the proposed boundary conditions (BC) here allowed us to investigate the adhesion of drug carriers with attention to the particular diffusivity of each type of ligand-receptor bond and study their role in the ultimate homogeneity of the adhered particles over the targeted endothelium.

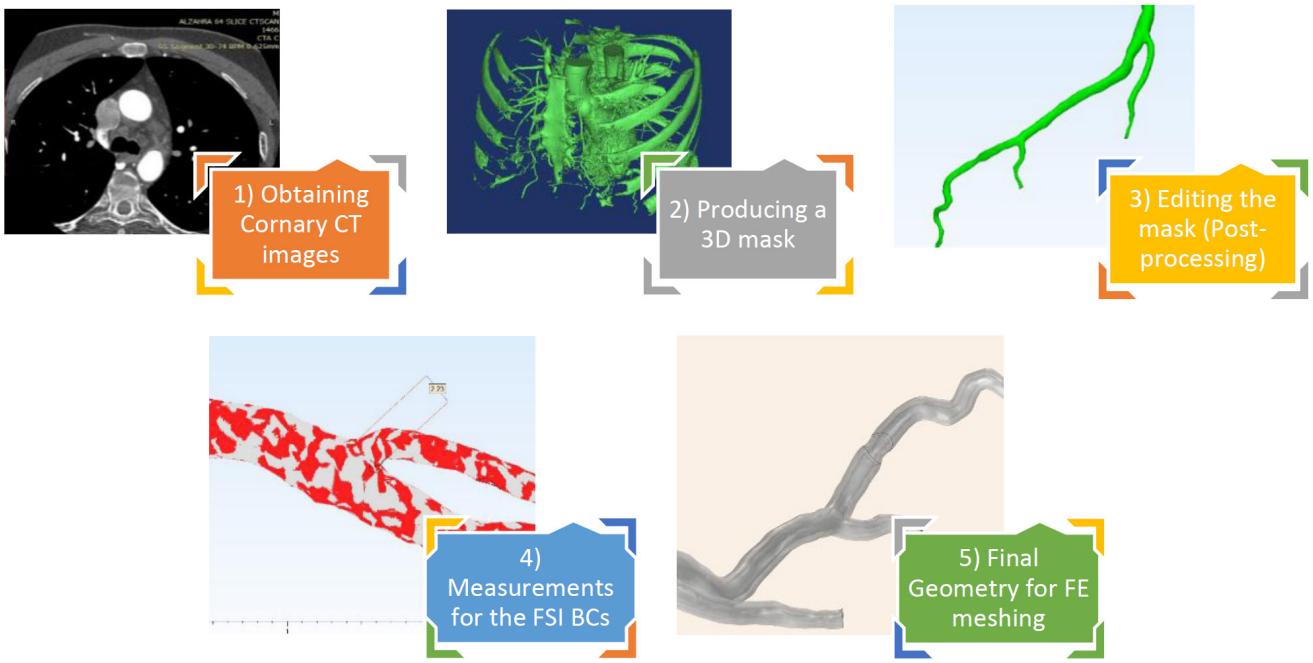

Fig. (1). The steps of reconstruction of the LAD arterial geometry. The CT scan images of a 51-year-old patient were obtained and used for image processing and segmentation to produce a 3D mask adopting a CT number thresholding method. Next, the 3D mask was manually edited and smoothed to eliminate the artefacts. Then, specific measurements were done to obtain the diameters of the inlet and outlets of the arterial geometry and the geometry of bifurcations. Ultimately, based on the 3D volume, the finite element meshable geometry was constructed [28]. (*A higher resolution / colour version of this figure is available in the electronic copy of the article*).

In several investigations, a connection between changes in the blood viscosity and cardiac pathological conditions such as hypertension and occlusion of vessels due to thromboses has been reported [18, 19]. Furthermore, diabetes, alongside prolonged tobacco smoking and high blood cholesterol, has been documented as autonomous risk factors for coronary diseases and the formation of atherosclerotic plaques [20, 21]. Ultimately, the blood haematocrit, as a primary influence on the blood viscosity, has specific links with the conditions [22, 23].

The present work offers a patient-specific isogeometric analysis of a reconstructed Left Anterior Descending (LAD) artery produced by image-processing of CT-Scan images. The patient's luminal unevenness and the precise position and structure of the constricting plaque are captured in the model. Fluid-Solid Interaction (FSI) analysis of the Non-Newtonian modelled blood flowing in the artery is made by employing the Finite Element Method (FEM). Then, in a convection-diffusion context, the distribution and delivery of particles in different diameters are investigated through an adapted receptor-mediated adhesion mechanism. In the present research, the adhesive dynamics of P-Selectin Aptamers (PSA), the ligands covering the surface of particles, regarding their unique biophysical features (the affinity, specific diffusivity, and reactive compliance) are simulated. Comparable to a number of the established multiscale approaches for drug delivery analysis [8, 24-27], our model incorporates the solutions from the FSI simulation in macroscale with the results of the micro/nanoscale model describing the particle movements and adhesion on the atherosclerotic plaque. Finally, the results were compared with the findings of previous relevant computational and experimental investigations.

2. MATERIALS AND METHODS

2.1. The Geometry Production

The exact geometry produced earlier [28] with the same consideration for Murray's law equation [29] has been used in this work. Detailed information on the reconstruction of the LAD geometry based on patient CT-Scan images has been given. The image-processing part gave us the FEM-solvable geometry of the LAD, which enabled us to perform isogeometric analyses for both FSI and transport of particles simulations. Fig. (**1**) shows the steps of building the LAD artery.

2.2. The Blood, The Vessel, and The Plaque Models

Since the pulsatility of physiological velocity waveforms in the coronary circulation and the nonlinearity of the geometry lead to momentous alterations in the blood shear rate, the blood was modelled an incompressible Non-Newtonian fluid using the Carreau-Yasuda equation (Eq. 1). Based on an experiment on viscosity data fittings for different pathological blood haematocrits [30], the values for parameters of

Eq. 1, given in Table **1**, have been selected. The viscosity of blood μ in this model is calculated as the following:

$$\mu = \mu_\infty + (\mu_0 - \mu_\infty)[1 + (\lambda\dot{\gamma})^2]^{(n-1)/2} \quad (1)$$

Where λ denotes the time constant, *n* represents the power-law index, ã˙ is the local shear-rate, μ0 and μ∞ denote zero-shear viscosity and infinite-shear viscosity, respectively.

Table 1. ***The parameters and corresponding values for the non-Newtonian Carreau-Yasuda blood model used in the FSI simulations*** **[30].**

Haematocrit (%)	μ_0 (Pa.s)	λ (s)	*n*	μ_∞ (Pa.s)
65	0.8592	103.088	0.389	0.00802

In this research, 65% of blood Haematocrit (Hct) was considered pathologically high, which can attribute to diseases such as diabetes or polycythaemia.

Similar to the previous work of the authors [28], the vessel wall was considered a single-layered, isotropic hyperelastic material. The details of the mechanical properties of the hyperelastic model and the values for the Mooney-Rivlin parameters have been found previously [28].

The exact atherosclerotic plaque model with the same mechanical characteristics and BCs employed earlier [28] was also used here. The position and form of the plaque in the LAD artery can be observed in the red ellipse in Fig. (**2**).

2.3. The BCs, The Governing Equations, and the Adhesion Model

The governing equations and boundary conditions for the FSI simulations have been discussed [24, 31]. Also, the transport of particles and the adhesive dynamic (AD) model are the same as described earlier [28]. Fig. (**2**) illustrates all the BCs used in the simulations, namely, physiological blood velocity waveform, the particle input release function, and the specific BC designed for the atherosclerotic plaque.

It should be noted that the ligands covering the surface of particles in this work are P-Selectin Aptamers (PSA). Thus, accordingly, the adhesion analysis will be done for PSA:P-selectin bonds. The values corresponding to the AD model for PSA:P-Selectin bindings have been selected from earlier work [28].

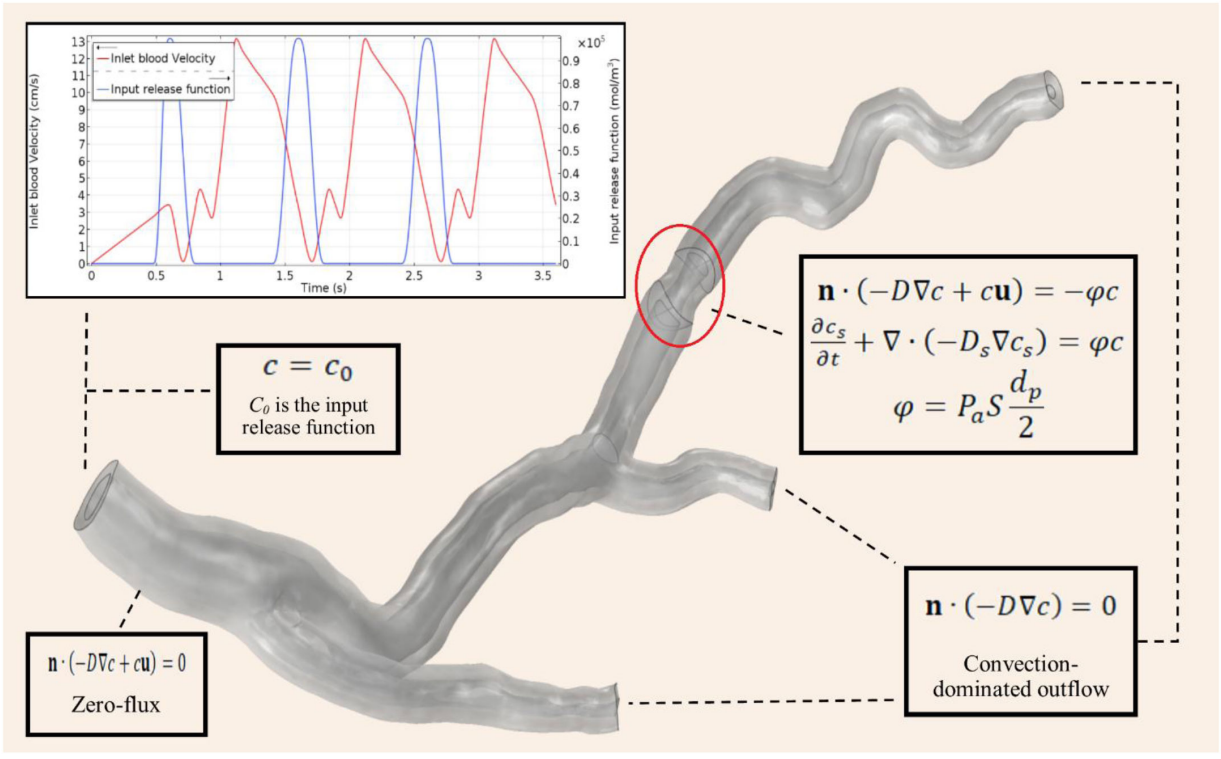

Fig. (2). The BCs applied in the flow and particle simulations. P_a indicates the adhesion strength calculated by AD model, S is the fluid shear rate, and d_p denotes the particle diameter. Also, n denotes the surface normal unit vector, c represents the concentration of nanoparticles in the blood domain, c_s denotes the concentration of adsorbed particles, u is the blood velocity vector, D represents the diffusion coefficient of particles, and D_s denotes the specific diffusivity of ligand-receptor bonds. (*A higher resolution / colour version of this figure is available in the electronic copy of the article*).

It is important to indicate that the particles were assumed to be injected into the blood flow in three shots starting at the opening of each cardiac cycle Fig. (**2**).

The homogeneity of attached particles over the surface of the plaque is studied *via* the variable *h,* which has been evaluated at the last time step (t = 3.6) and formulated as:

$$h = \sqrt{(g\_cx)^2 + (g\_cy)^2 + (g\_cz)^2} \quad (2)$$

Where g_cs represent the concentration gradients in Cartesian directions. For the simulation setup and information of used solvers, earlier research has been used [28].

3. RESULTS AND DISCUSSION

The Surface Density of Adhered particles (SDA) on the atherosclerotic plaque was calculated for different particle diameters in high blood Hct. The results were compared to their counterparts obtained in normal (healthy) blood Hct [28].

As Fig. (**3**) shows, unlike the healthy Hct results, from 800 to 1600 nm of diameter, the change in SDA was insignificant. In high Hct, the SDA for 200 nm particles is 9.06% smaller compared to the average SDA of other particle sizes. In drug carrier design protocols designed for targeting an atherosclerotic plaque in pathologically high blood haematocrits, it is insightful to consider that increasing the carrier size, from near micron onwards, might have a trivial effect on the surface density of adhered particles over the targeted endothelium. When drug receivers have high Hct blood-related diseases, the drug carrier designers can have flexible options if they tend to use micron-sized carriers. However, if the addressees have normal blood Hct (45% in this study) increase in the particle size results in the higher SDAs over the plaque surface. It becomes particularly significant for over micron-sized particles.

Also, the Homogeneity Indices (*h*) were obtained for particles of different diameters in high Hct blood flow simulated in this work and were compared with the particles adsorbed over the same atherosclerotic plaque in normal blood Hct [28].

The homogeneity index, *h*, represents the concentration gradient over the plaque surface. Smaller *h* denotes more homogenous adsorption of particles. As can be seen in Fig. (**4**), overall, particles adhere more homogenously on the targeted endothelium when travelling in the high blood Hpc. Again, the alteration in *h* is minor from 800 to 3200 nm particles simulated in the high Hct blood.

Finally, Fig. (**5**) illustrates the deposition maps for 800 nm particles simulated in normal and high blood Hcts. Not only does it confirm the homogeneity evaluation done for these particles Fig. (**4**), but also it indicates that the high Hct blood flow interestingly affects the adsorption pattern over the plaque surface. Particularly, Fig. (**5**) shows a significant area of deposited particles in the post-constriction region, a phenomenon that does not occur when particles are delivered in the normal Hct blood flow.

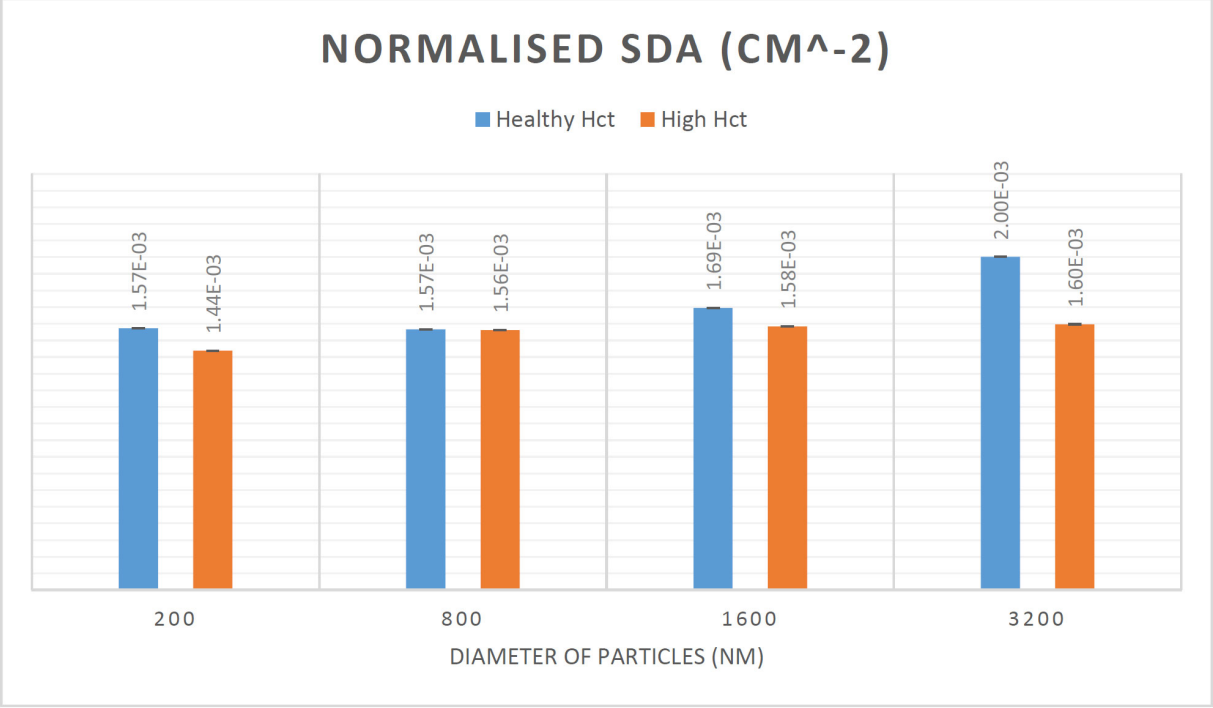

Fig. (3). Distribution of Normalised SDAs based on the particle diameter. Error bars are standard deviations. (*A higher resolution / colour version of this figure is available in the electronic copy of the article*).

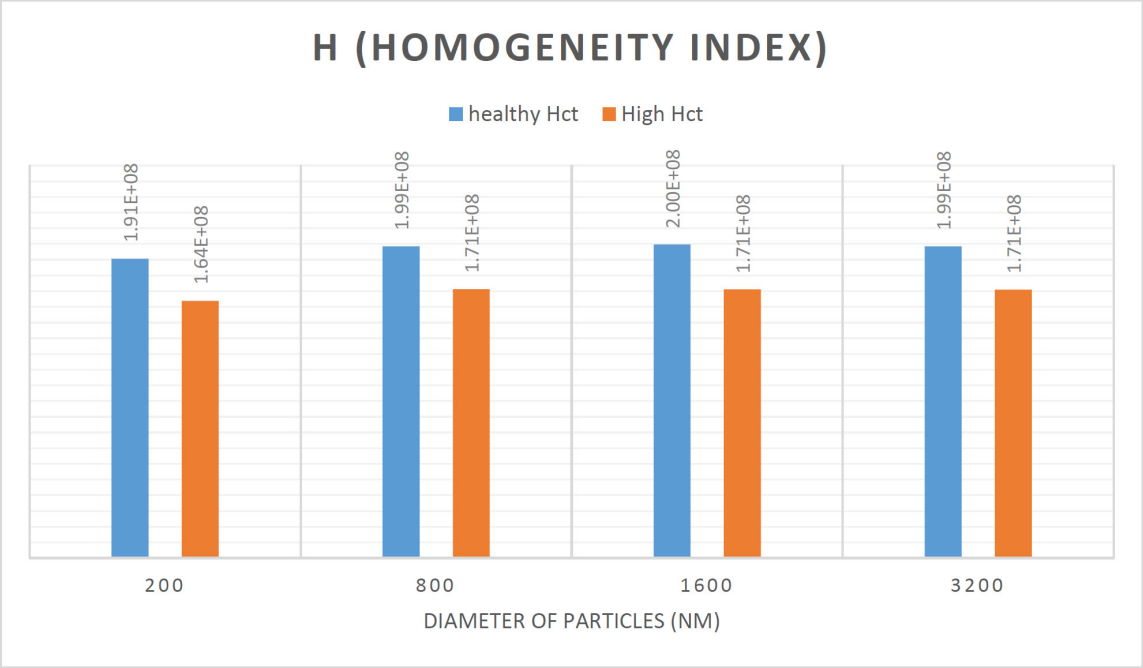

Fig. (4). Distribution of homogeneity index for the different diameters of particles in healthy and high Hcts. (*A higher resolution / colour version of this figure is available in the electronic copy of the article*).

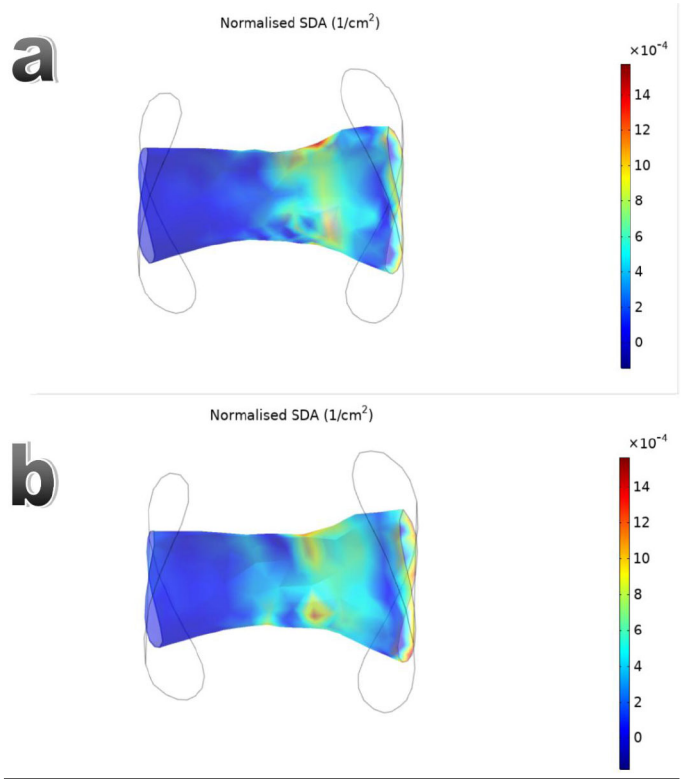

Fig. (5). Deposition maps of 800 nm particles simulated in (a) normal (45%) blood Hct and (b) High (65%) blood Hct. (*A higher resolution / colour version of this figure is available in the electronic copy of the article*).

To elucidate, the increase in particle size in normal blood Hct results in an upsurge in the surface density of adhered particles over the plaque. This occurs since the surface deposition variable ö in Fig. (**2**) defined over the atherosclerotic plaque is directly proportional to particle diameter dp. Therefore, the increase in particle size will result in stronger deposition flux towards the surface of the plaque, thus increasing the SDA. This finding is in accord with recent investigations on particle margination in the LAD artery and microcirculation [28, 32, 33].

On the other hand, particles in high Hct have been observed with more homogenous deposition over the particle surface and lower or equal SDAs compared to the same particles in the normal Hct. The authors believe that the higher fluid viscous stress at the constriction domain in high blood Hct (also reported earlier [24]) intensifies the mixture of blood and diluted concentration of particles, thus leading to a more homogenous adhesion pattern over the plaque. A previous experimental study indicates that high blood Hct elicited significantly higher particle dispersion in a capillary tube compared to a normal flow [34].

CONCLUSION

The transport and adhesion of nanoparticles covered with PSA over the surface of a LAD atherosclerotic plaque were simulated in a pathologically high blood Hct. The role of particle diameter in the final surface density of adhered carriers and their deposition homogeneity was investigated. The distribution of adhered particles over the plaque, which travelled in high Hct blood, was significantly more homogenous than that of particles in normal blood Hct. The authors infer that this phenomenon might correlate with the high fluid viscous stresses at the plaque domain, which results in the intensified mixture at the plaque domain in high blood Hct.

On the other hand, the SDA of particles in both blood haematocrits was elevated by increasing the particle size. Notably, in normal Hct, increasing the particle size from 200 to 800 nm had an insignificant effect on the increase in the SDAs over the targeted endothelium. Also, in high Hct, for 800 nm particles forwards, the change in SDA due to the increase in particle size was insignificant. However, in normal blood Hct (45% assumed in this study), the largest studied particle size resulted in the highest SDA over the plaque. It must be remembered that the results and discussions in the present research are under the influence of pathological patient-specific features (constricted lumen, geometry and location of the plaque, and luminal unevenness). Finally, the results obtained in normal and high blood Hct were verified against the results of pertinent experimental and computational studies.

ETHICS APPROVAL AND CONSENT TO PARTICIPATE

Not applicable.

HUMAN AND ANIMAL RIGHTS

No animals/humans were used for studies that are the basis of this research.

CONSENT FOR PUBLICATION

Not applicable.

AVAILABILITY OF DATA AND MATERIALS

The data supporting the findings of the article are available in the electronic supplementary material at [https://link.springer.com/article/10.1007/s10237-018-01116-y#Sec15], reference number [28]. The setup simulation files can be provided by the corresponding author [Amir Shamloo] upon reasonable request.

FUNDING

None.

CONFLICT OF INTEREST

The authors declare no conflict of interest, financial or otherwise.

ACKNOWLEDGEMENTS

The authors wish to express appreciation to Dr. Amirreza Sajjadieh for his clinical insight and expertise, which enriched this work.

REFERENCES

[1] Maul, T.M.; Dudgeon, D.D.; Beste, M.T.; Hammer, D.A.; Lazo, J.S.; Villanueva, F.S.; Wagner, W.R. Optimization of ultrasound contrast agents with computational models to improve selection of ligands and binding strength. *Biotechnol. Bioeng.,* **2010**, *107*(5), 854-864. http://dx.doi.org/10.1002/bit.22857 PMID: 20665479

[2] Villanueva, F.S.; Lu, E.; Bowry, S.; Kilic, S.; Tom, E.; Wang, J.; Gretton, J.; Pacella, J.J.; Wagner, W.R. Myocardial ischemic memory imaging with molecular echocardiography. *Circulation,* **2007**, *115*(3), 345-352. http://dx.doi.org/10.1161/CIRCULATIONAHA.106.633917 PMID: 17210843

[3] Kaufmann, B.A.; Sanders, J.M.; Davis, C.; Xie, A.; Aldred, P.; Sarembock, I.J.; Lindner, J.R. Molecular imaging of inflammation in atherosclerosis with targeted ultrasound detection of vascular cell adhesion molecule-1. *Circulation,* **2007**, *116*(3), 276-284. http://dx.doi.org/10.1161/CIRCULATIONAHA.106.684738 PMID: 17592078

[4] Khodabandehlou, K.; Masehi-Lano, J.J.; Poon, C.; Wang, J.; Chung, E.J. Targeting cell adhesion molecules with nanoparticles using *in vivo* and flow-based *in vitro* models of atherosclerosis. *Exp. Biol. Med. (Maywood),* **2017**, *242*(8), 799-812. http://dx.doi.org/10.1177/1535370217693116 PMID: 28195515

[5] Muzykantov, V.R. Targeted Drug Delivery to Endothelial Adhesion Molecules, ISRN. *Vasc. Med.,* **2013**, *2013*, 1-27. http://dx.doi.org/10.1155/2013/916254

[6] Weller, G.E.; Lu, E.; Csikari, M.M.; Klibanov, A.L.; Fischer, D.; Wagner, W.R.; Villanueva, F.S. Ultrasound imaging of acute cardiac transplant rejection with microbubbles targeted to intercellular adhesion molecule-1. *Circulation,* **2003**, *108*(2), 218-224. http://dx.doi.org/10.1161/01.CIR.0000080287.74762.60 PMID: 12835214

[7] Ghosh, S.; Matsuoka, Y.; Asai, Y.; Hsin, K.Y.; Kitano, H. Software for systems biology: from tools to integrated platforms. *Nat. Rev. Genet.,* **2011**, *12*(12), 821-832.

http://dx.doi.org/10.1038/nrg3096 PMID: 22048662

[8] Hossain, S.S.; Zhang, Y.; Liang, X.; Hussain, F.; Ferrari, M.; Hughes, T.J.; Decuzzi, P. *In silico* vascular modeling for personalized nanoparticle delivery. *Nanomedicine (Lond.),* **2013**, *8*(3), 343-357.
http://dx.doi.org/10.2217/nnm.12.124 PMID: 23199308

[9] Nie, S. Nanotechnology for personalized and predictive medicine, Nanomedicine Nanotechnology. *Biol. Med.*, **2006**, *2*
http://dx.doi.org/10.1016/j.nano.2006.10.115

[10] Vizirianakis, I.S. *Handbook of Personalized Medicine: Advances in Nanotechnology*; Drug Delivery, and Therapy: Pan Stanford, New York, **2014**.
http://dx.doi.org/10.1201/b15465

[11] Forouzandehmehr, M.; Cogno, N.; Koivumäki, J.; Hyttinen, J.; Paci, M. The Comparison Between Two Mathematical Contractile Elements Integrated into an hiPSC-CM In-silico Model In: *Comput. Cardiol*; , **2020**.
http://dx.doi.org/10.22489/CinC.2020.055

[12] Shamloo, A.; Manuchehrfar, F.; Rafii-Tabar, H. A viscoelastic model for axonal microtubule rupture. *J. Biomech.,* **2015**, *48*(7), 1241-1247.
http://dx.doi.org/10.1016/j.jbiomech.2015.03.007 PMID: 25835789

[13] Shamloo, A.; Mohammadaliha, N.; Mohseni, M. Integrative Utilization of Microenvironments, Biomaterials and Computational Techniques for Advanced Tissue Engineering. *J. Biotechnol.,* **2015**, *212*, 71-89.
http://dx.doi.org/10.1016/j.jbiotec.2015.08.005 PMID: 26281975

[14] Shamloo, A.; Pedram, M.Z.; Heidari, H.; Alasty, A. Computing the blood brain barrier (BBB) diffusion coefficient: A molecular dynamics approach. *J. Magn. Magn. Mater.,* **2016**.
http://dx.doi.org/10.1016/j.jmmm.2016.03.030

[15] Amr, A.; Kayvanpour, E.; Sedaghat-Hamedani, F.; Passerini, T.; Mihalef, V.; Lai, A.; Neumann, D.; Georgescu, B.; Buss, S.; Mereles, D.; Zitron, E.; Posch, A.E.; Würstle, M.; Mansi, T.; Katus, H.A.; Meder, B. Personalized Computer Simulation of Diastolic Function in Heart Failure. *Genomics Proteomics Bioinformatics,* **2016**, *14*(4), 244-252.
http://dx.doi.org/10.1016/j.gpb.2016.04.006 PMID: 27477449

[16] Itu, L.M.; Sharma, P.; Suciu, C. Patient-specific Hemodynamic Computations: Application to Personalized Diagnosis of Cardiovascular Pathologies **2017**.
http://dx.doi.org/10.1007/978-3-319-56853-9

[17] Kayvanpour, E.; Mansi, T.; Sedaghat-Hamedani, F.; Amr, A.; Neumann, D.; Georgescu, B.; Seegerer, P.; Kamen, A.; Haas, J.; Frese, K.S.; Irawati, M.; Wirsz, E.; King, V.; Buss, S.; Mereles, D.; Zitron, E.; Keller, A.; Katus, H.A.; Comaniciu, D.; Meder, B. Towards Personalized Cardiology: Multi-Scale Modeling of the Failing Heart. *PLoS One,* **2015**, *10*(7), e0134869.
http://dx.doi.org/10.1371/journal.pone.0134869 PMID: 26230546

[18] Letcher, R.L.; Chien, S.; Pickering, T.G.; Laragh, J.H. Elevated blood viscosity in patients with borderline essential hypertension. *Hypertension,* **1983**, *5*(5), 757-762.https://www.ncbi.nlm.nih.gov/pubmed/6352482
http://dx.doi.org/10.1161/01.HYP.5.5.757 PMID: 6352482

[19] Lowe, G.D. Blood rheology in arterial disease. *Clin. Sci. (Lond.),* **1986**, *71*(2), 137-146.https://www.ncbi.nlm.nih.gov/pubmed/3522049
http://dx.doi.org/10.1042/cs0710137 PMID: 3522049

[20] Colwell, J.A.; Lopes-Virella, M.; Halushka, P.V. Pathogenesis of atherosclerosis in diabetes mellitus. *Diabetes Care,* **1981**, *4*(1), 121-133.https://www.ncbi.nlm.nih.gov/pubmed/7009108
http://dx.doi.org/10.2337/diacare.4.1.121 PMID: 7009108

[21] Sarnak, M.J.; Tighiouart, H.; Manjunath, G.; MacLeod, B.; Griffith, J.; Salem, D.; Levey, A.S. Anemia as a risk factor for cardiovascular disease in The Atherosclerosis Risk in Communities (ARIC) study. *J. Am. Coll. Cardiol.,* **2002**, *40*(1), 27-33.
http://dx.doi.org/10.1016/S0735-1097(02)01938-1 PMID: 12103252

[22] Pries, A.R.; Neuhaus, D.; Gaehtgens, P. Blood viscosity in tube flow: dependence on diameter and hematocrit. *Am. J. Physiol.,* **1992**, *263*(6 Pt 2), H1770-H1778.https://www.ncbi.nlm.nih.gov/pubmed/1481902
PMID: 1481902

[23] Stadler, A.A.; Zilow, E.P.; Linderkamp, O. Blood viscosity and optimal hematocrit in narrow tubes. *Biorheology,* **1990**, *27*(5), 779-788.https://www.ncbi.nlm.nih.gov/pubmed/2271768
http://dx.doi.org/10.3233/BIR-1990-27513 PMID: 2271768

[24] Forouzandehmehr, M.; Shamloo, A. Margination and adhesion of micro- and nanoparticles in the coronary circulation: a step towards optimised drug carrier design. *Biomech. Model. Mechanobiol.,* **2018**, *17*(1), 205-221.
http://dx.doi.org/10.1007/s10237-017-0955-x PMID: 28861632

[25] Sohrabi, S.; Wang, S.; Tan, J.; Xu, J.; Yang, J.; Liu, Y. Nanoparticle transport and delivery in a heterogeneous pulmonary vasculature. *J. Biomech.,* **2017**, *50*, 240-247.
http://dx.doi.org/10.1016/j.jbiomech.2016.11.023 PMID: 27863742

[26] Tan, J.; Wang, S.; Yang, J.; Liu, Y. Coupled Particulate and Continuum Model for Nanoparticle Targeted Delivery. *Comput. Struc.,* **2013**, *122*, 128-134.
http://dx.doi.org/10.1016/j.compstruc.2012.12.019 PMID: 23729869

[27] Amani, A.; Shamloo, A.; Barzegar, S.; Forouzandehmehr, M. Effect of Material and Population on the Delivery of Nanoparticles to an Atherosclerotic Plaque: A Patient-specific *In Silico* Study. *Langmuir,* **2021**, *37*(4), 1551-1562.
http://dx.doi.org/10.1021/acs.langmuir.0c03158 PMID: 33465311

[28] Shamloo, A.; Forouzandehmehr, M. Personalised deposition maps for micro- and nanoparticles targeting an atherosclerotic plaque: attributions to the receptor-mediated adsorption on the inflamed endothelial cells. *Biomech. Model. Mechanobiol.,* **2019**, *18*(3), 813-828.
http://dx.doi.org/10.1007/s10237-018-01116-y PMID: 30617526

[29] van der Giessen, A.G.; Groen, H.C.; Doriot, P.A.; de Feyter, P.J.; van der Steen, A.F.; van de Vosse, F.N.; Wentzel, J.J.; Gijsen, F.J. The influence of boundary conditions on wall shear stress distribution in patients specific coronary trees. *J. Biomech.,* **2011**, *44*(6), 1089-1095.
http://dx.doi.org/10.1016/j.jbiomech.2011.01.036 PMID: 21349523

[30] Kwon, O.; Krishnamoorthy, M.; Cho, Y.I.; Sankovic, J.M.; Banerjee, R.K. Effect of blood viscosity on oxygen transport in residual stenosed artery following angioplasty. *J. Biomech. Eng.,* **2008**, *130*(1), 011003.
http://dx.doi.org/10.1115/1.2838029 PMID: 18298179

[31] Shamloo, A.; Amani, A.; Forouzandehmehr, M.; Ghoytasi, I. *In silico* study of patient-specific magnetic drug targeting for a coronary LAD atherosclerotic plaque. *Int. J. Pharm.,* **2019**, *559*, 113-129.
http://dx.doi.org/10.1016/j.ijpharm.2018.12.088 PMID: 30654060

[32] Müller, K.; Fedosov, D.A.; Gompper, G. Margination of micro- and nano-particles in blood flow and its effect on drug delivery. *Sci. Rep.,* **2014**, *4*, 4871.
http://dx.doi.org/10.1038/srep04871 PMID: 24786000

[33] Müller, K.; Fedosov, D.A.; Gompper, G. Understanding particle margination in blood flow - A step toward optimized drug delivery systems. *Med. Eng. Phys.,* **2016**, *38*(1), 2-10.
http://dx.doi.org/10.1016/j.medengphy.2015.08.009 PMID: 26343228

[34] Saadatmand, M.; Ishikawa, T.; Matsuki, N.; Jafar Abdekhodaie, M.; Imai, Y.; Ueno, H.; Yamaguchi, T. Fluid particle diffusion through high-hematocrit blood flow within a capillary tube. *J. Biomech.,* **2011**, *44*(1), 170-175.
http://dx.doi.org/10.1016/j.jbiomech.2010.09.004 PMID: 20887991